Modulation of Transgene Expression in Retinal Gene Therapy by Selective Laser Treatment

Daniel Lavinsky,[1–3] *Thomas W. Chalberg,*[4] *Yossi Mandel,*[1,2] *Philip Huie,*[1,2] *Roopa Dalal,*[1] *Michael Marmor,*[1] *and Daniel Palanker*[1,2]

Purpose. To develop a method for modulation of transgene expression in retinal pigment epithelium (RPE) using scanning laser that spares neurosensory retina.

Methods. Fifteen pigmented rabbits received subretinal injection of recombinant adeno-associated virus (rAAV-2) encoding green fluorescent protein (GFP). GFP expression was measured using confocal scanning laser ophthalmoscopy (cSLO) fluorescence imaging and immunohistochemistry. To reduce the total expression in RPE by half, 50% of the transfected RPE cells were selectively destroyed by microsecond exposures to scanning laser with 50% pattern density. The selectivity of RPE destruction and its migration and proliferation were monitored using fluorescein angiography, spectral-domain optical coherence tomography (SD-OCT), and light, transmission, and scanning electron microscopy. 5-Bromo-2′-dioxyuridine (BrdU) assay was performed to evaluate proliferation of RPE cells.

Results. RPE cells were selectively destroyed by the line scanning laser with 15 μs exposures, without damage to the photoreceptors or Bruch's membrane. RPE cells started migrating after the first day, and in 1 week there was complete restoration of RPE monolayer. Selective laser treatment decreased the GFP fluorescence by 54% as compared to control areas; this was further decreased by an additional 48% following a second treatment 1 month later. BrdU assay demonstrated proliferation in approximately half of the RPE cells in treatment areas.

Conclusions. Microsecond exposures produced by scanning laser destroyed RPE cells selectively, without damage to neural retina. Continuity of RPE layer is restored within days by migration and proliferation, but transgene not integrated into the nucleus is not replicated. Therefore, gene expression can be modulated in a precise manner by controlling the laser pattern density and further adjusted using repeated applications. (*Invest Ophthalmol Vis Sci.* 2013;54:1873–1880) DOI: 10.1167/iovs.12-10933

From the Department of [1]Ophthalmology and the [2]Hansen Experimental Physics Laboratory, Stanford University, Stanford, California; the [3]Federal University of São Paulo (UNIFESP), São Paulo, Brazil; and [4]Avalanche Biotechnologies, Inc., San Francisco, California.

Supported by the 2012 Guillingham Pan-American Fellowship, Pan-American Ophthalmological Foundation, and Retina Research Foundation (DL).

Submitted for publication September 9, 2012; revised November 18, 2012 and February 5, 2013; accepted February 9, 2013.

Disclosure: **D. Lavinsky**, Topcon Medical Laser Systems (TMLS) (C); **T.W. Chalberg**, Avalanche Biotechnologies, Inc. (I, E); **Y. Mandel**, None; **P. Huie**, None; **R. Dalal**, None; **M. Marmor**, None; **D. Palanker**, TMLS (I, C), Avalanche Biotechnologies, Inc. (I), P

Corresponding author: Daniel Lavinsky, 452 Lomita Mall, Room 141, Stanford, CA 94305; Daniellavinsky@gmail.com.

The recent demonstration of safety and efficacy in human trials has ushered in a new era of promise for gene therapy of retinal diseases.[1] Clinical experience with an adeno-associated viral vector for Leber congenital amaurosis (LCA) has already demonstrated safety of retinal gene therapy[2–4] and sustained visual improvement.[4] Additional programs are advancing toward the clinic or are in ongoing clinical trials, including the treatment of age-related macular degeneration (AMD),[5,6] retinitis pigmentosa, retinoschisis, and Stargardt's disease.[7]

Gene therapy for retinal neovascular diseases, which affect a large and growing population, are of specific interest because of the high prevalence of these diseases and the high burden of care under current therapeutic regimens. AMD is the leading cause of visual loss in patients > 50 years old, with 7.5 million people likely to be affected by AMD-related visual impairment in the United States by 2020.[8] The current standard of care for treatment of wet AMD is frequent (often monthly) intravitreal injections of agents such as bevicizumab, ranibizumab (Lucentis), or, more recently, aflibercept (VEGF-trap).[9] These molecules inhibit VEGF signaling, thereby slowing progression of neovascularization and reducing macular edema. Frequent injections are burdensome for patients and physicians, are associated with very high cost to the health care system, and carry cumulative risk of ocular infection with potentially devastating consequences. In 2009, well over a million (1,270,836) intravitreal injections for eye diseases cost Medicare and Medicaid more than $2 billion, an amount that is expected to grow rapidly as more indications are approved and the population ages. Such an immense financial burden on health care and patients signifies an urgent need to develop more cost-effective treatments for retinal diseases.

Gene therapy may allow viral transfection of ocular cells to create a "biofactory" that secretes therapeutic agents within the eye, eliminating the need for monthly injections. The leading program in development uses recombinant adeno-associated virus (rAAV-2) encoding for sFlt-1, which is a highly potent and naturally occurring antiangiogenic peptide that binds and inactivates VEGF. Subretinal delivery of rAAV.sFlt-1 prevents and reverses progression of ocular neovascularization in mice and nonhuman primates,[5] and is currently the subject of a Phase 1/2 clinical trial for wet AMD (NCT01494805). In the longer term, AMD could also be addressed by treatments that target the complement pathway, as several complement proteins have been implicated in AMD.[10]

One challenge for genetic therapy is the need to downregulate gene expression in the case of total resolution of disease or adverse reaction to the therapy.[11,12] Several systems have been designed to address this concern.[13] Some use an inducible system, in which a small molecule such as doxycycline modulates a transcription factor regulatory domain and keeps transgene expression on (Tet-On system) or off (Tet-Off system).[11] Other systems involve inducers such as rapamycin,[14] mifepristone (RU-486),[15] and the ecdysone

receptor from *Drosophila melanogaster*.[16] The most widely used systems require that a drug be taken on a constant basis to maintain expression in the "on" or "off" state.[11,12] However, these drugs may have undesirable side effects, such as immunosuppression with rapamycin, and off-target effects of steroid hormones.[15] Systems that seem to avoid this problem, such as the Tet-On, suffer from an immune response to the gene product.[17]

The primary target for genetic therapy of AMD and many other retinal diseases is the RPE, a supportive monolayer of cells underneath the neural retina. We have developed a method for downregulation of the transgene expression in RPE that selectively destroys a designated fraction of RPE cells using a rapidly scanning laser. Microsecond pulses of light vaporize the melanosomes and thereby destroy RPE cells while minimizing heat diffusion into the surrounding Bruch's membrane and neural retina.[18] Continuity of the RPE layer is restored by migration and proliferation of adjacent RPE cells, and the photoreceptors rapidly recover. However, with vector systems such as AAV in which the transgene is not replicated, the vector is lost in dividing cells, leading to a decrease in transgene expression. Thus by selective destruction of transfected cells followed by stimulated cell division, transgene expression can be precisely decreased by controlling the level of selective cell destruction via the laser pattern density applied.

Methods

Animals

Fifteen Dutch Belted rabbits (weight, 1.5–2.5 kg) were used in accordance with the ARVO Statement for the Use of Animals in Ophthalmic and Vision Research, after approval from the Stanford University Animal Institutional Review Board. The rabbits were anesthetized using ketamine hydrochloride (35 mg/kg), xylazine (5 mg/kg), and glycopyrrolate (0.01 mg/kg) administered intramuscular (IM) 15 minutes before the procedure. Pupillary dilation was achieved by one drop each of 1% tropicamide and 2.5% phenylephrine hydrochloride. One drop of topical tetracaine 0.5% was instilled in each eye before treatment.

Scanning Laser System

A 532 nm laser (PASCAL; Topcon Medical Laser Systems, Santa Clara, CA) provided a beam with top-hat intensity profile.[19] The software controlling the system (PASCAL; Topcon Medical Laser Systems) was modified for rapid scanning of the laser to achieve microsecond dwell times, with a scanning speed up to 6.6 m/s. The custom graphical user interface allowed adjusting the laser power, scanning velocity, number of lines in the pattern, and spacing between the lines. Once the treatment parameters were appropriately selected, a foot pedal was used to activate the laser.[20]

To limit laser damage to just the RPE cells, the laser exposure time must be in the range of microseconds.[18,20,21] For a given target size L, the thermal confinement time $t = L^2/4\alpha$, where α is the thermal diffusivity of tissue. For example, for the apical melanin layer in RPE cells, $L \approx 4$ μm, and $t \approx 28$ μs in water. Microsecond exposures can be produced efficiently with a continuous laser[20,21] that is rapidly scanned across the tissue. Exposure time is determined by the laser spot size divided by the scanning speed. For example, with a beam diameter of 100 μm and a velocity of 6.6 m/s, the exposure duration on an RPE cell is only 15 μs.

A Mainster wide-field retinal laser contact lens (Ocular Instruments, Bellevue, WA) was used to focus the laser on the rabbit fundus, providing the retinal spot size in a rabbit eye equal to the aerial diameter. Using the line scanning software (PASCAL; Topcon Medical Laser Systems), line patterns were applied in triple lines separated by one line diameter (50% coverage) using 100 μm spot size. Power was titrated to a level that produced a burn invisible clinically and in optical coherence tomography (OCT), but visible in fluorescein angiography. Further histologic and transmission electron microscopy (TEM) analysis confirmed that this method of titration was reliable for producing damage limited to the RPE with no or minimal effect on outer segments. Power ranged from 1.1 to 1.3 W with scanning velocity of 6 m/s.

Viral Vectors

Recombinant AAV serotype 2 expressing green fluorescent protein (GFP) under control of the citomegalovirus (CMV)-IE promoter (Virovek, Inc., Hayward, CA) was produced as described previously.[21] The rAAV.GFP was titered using real-time polymerase chain reaction (qPCR) and diluted to 1×10^{12} vg/mL, stored at –80°C, and thawed immediately prior to injection. Subretinal AAV has been extensively studied in the retina and RPE, including in mice,[22–24] rats,[25,26] dogs,[27–30] nonhuman primates,[5,23] and humans[31–34] and more recently also in rabbit retina.[35] The vector titer in our study was determined based on previous publications, which used concentrations similar to those applied subretinally in most recent clinical trials.[31]

Subretinal Injection of rAAV2.GFP

Six eyes of six rabbits were used for subretinal injection of rAAV2.GFP. A transconjunctival 25-gauge trocar cannula (Alcon, Fort Worth, TX) was inserted through the sclera 3 mm from the corneoscleral limbus at a steep angle to avoid the lens, and the trocar was removed leaving the cannula in place. Partial posterior vitrectomy was performed, and a 25 and 41G extendable cannula (DORC, Inc., Exeter, NH) was used to inject 50 μL fluid into the subretinal space, creating three blebs per eye: two with the viral vector and one reference bleb with vehicle alone (balanced salt solution [BSS]; Alcon). OCT was used to confirm the presence of subretinal bleb. Sclerotomy was closed with 7-0 Vicryl sutures (Ethicon, Somerville, NJ). After surgery, animals received atropine eye drops, subconjunctival triamcinolone (Bristol-Myers Squibb, New York, NY), and corneal application of ointment containing bacitracin zinc (500 U/g) and polymixin B sulfate (10,000 U/g; Akorn, Lake Forest, IL). No detrimental effects were seen from the AAV or GFP expression, with the exception of a visible mark at the site of retinotomy, which was also associated with increased autofluorescence.

In Vivo Imaging

To study dynamics of RPE healing after laser treatment, 15 eyes with no prior surgery were submitted to the same scanning laser protocol at 2 months, 1 month, 1 week, 3 days, 1 day, and 1 hour before enucleation. Confocal scanning laser ophthalmoscopy (cSLO) and OCT imaging was used at each time point. At 2 months, rabbits were euthanized as described previously, and eyes were processed for either light and TEM or scanning electron microscopy.

After surgery, rabbits were followed weekly with cSLO autofluorescence mode and OCT (HRA2-Spectralis; Heidelberg Engineering, Heidelberg, Germany). One transfected bleb in each eye was randomly selected for laser, and one received no laser treatment as a control. After laser treatment at 3 weeks postinjection, imaging was performed at 1 day, and then again at weekly intervals. One month after the first laser treatment, blebs were treated again with the same laser parameters and followed for additional 3 weeks until the animals were euthanized for tissue analysis.

For fluorescence imaging, animals were anesthetized and their pupils dilated as described earlier. A cSLO with a 488 nm blue excitation and 500 nm green emission filter (autofluorescence mode) was used for fluorescence measurements. At least five images of each bleb were captured, and total brightness was quantified using ImageJ

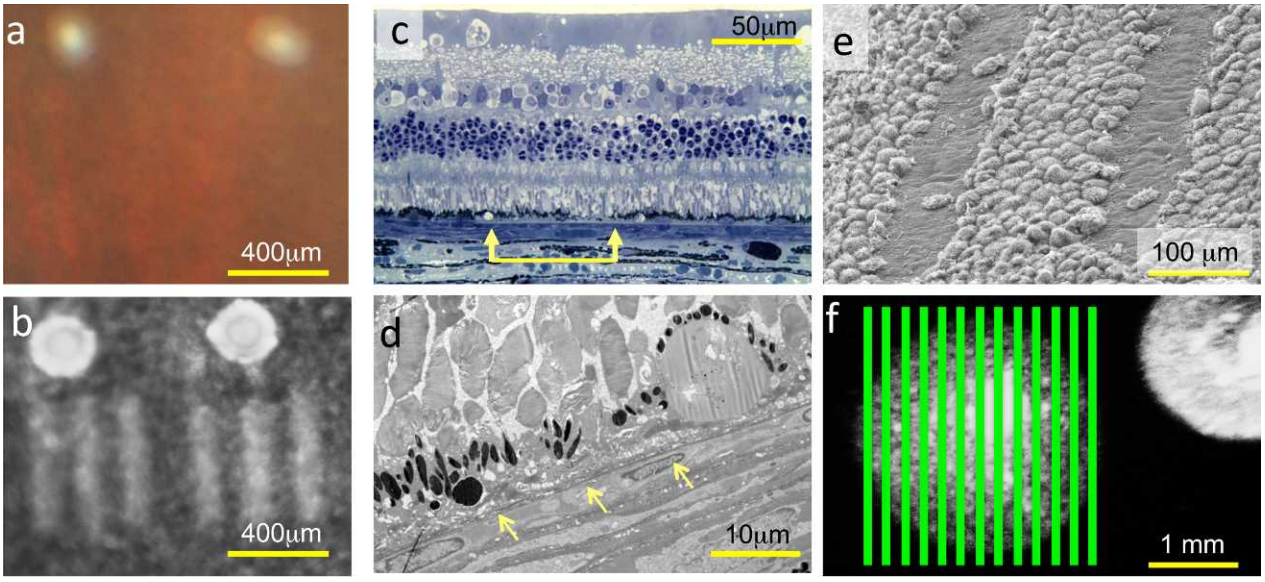

Figure 1. (**a**) Color fundus picture within 1 hour of the treatment shows marker burns and no visible signs of laser scanning pattern. (**b**) Fundus angiography shows hyperfluorescent lines where the laser was applied. (**c**) Light microscopy (LM) of acute lesion shows collapsed RPE cells with decreased melanin content (*yellow arrows*) and no damage to photoreceptors and choroid underneath. (**d**) Transmission electron microscopy (TEM) of the treated zone shows vacuolization of RPE cells and no damage to Bruch's membrane (*arrows*) or choriocapillaris. (**e**) Scanning electron microscopy (SEM) of the RPE cell layer at 1 day demonstrates the absence of RPE cells in the line scanning pattern. (**f**) Diagram of the laser pattern applied to the GFP-transfected bleb.

software (National Institutes of Health, Bethesda, MD). Data from each bleb were normalized to 21 days brightness, which represented the maximum expression before the laser treatment. The ratio of the signals from the treated and control blebs, with subtracted autofluorescent background, was calculated for each eye. Real-time eye tracking enabled averaging of multiple scans to reduce speckle noise and ensured that the images were acquired at the same locations, improving reliability of the follow-up.

Retinal Histology

Eyes were enucleated and fixed in 1.25% glutaraldehyde/1% paraformaldehyde in cacodylate buffer at pH 7.2 overnight at room temperature. The tissue was then postfixed in osmium tetroxide, dehydrated with a graded series of ethanol, and processed with propylene oxide. Tissue was embedded into epoxy resin (EMbed 812; Electron Microscopy Sciences, Port Washington, PA). One-micrometer sections for light microscopy or 100 nm sections for TEM were cut on an ultramicrotome (Reichert-Jung Ultracut E; Leica, Deerfield, IL). Sections for light microscopy were stained with toluidine blue and photographed on a light microscope (Eclipse E1000; Nikon, Tokyo, Japan). Thin sections for electron microscopy were stained with uranyl acetate and lead citrate. Transmission electron micrographs were captured with a JEM-1400 (JEOL USA, Inc., Peabody, MA).

Scanning Electron Microscopy

For scanning electron microscopy (SEM), six eyes were enucleated rapidly; the anterior segment of the globe was incised and separated from the posterior part of the eye cup; and retina was manually peeled from the RPE. The remaining sclera, choroid, and RPE were fixed in glutaraldehyde–paraformaldehyde fixative (1.25%/1% in 0.2 M sodium cacodylate buffer) at room temperature for 30 minutes. The tissue was then fixed for an additional 18 hours at 4°C, rinsed in a buffer, and postfixed in 1% osmium tetroxide in 0.2 M sodium cacodylate, pH 7.4. The tissue was washed with distilled water, dehydrated in a series of ethanols, transferred to absolute ethanol, and critical point dried. The dried tissues were then mounted on stubs and plasma coated with gold/palladium (Denton Vacuum, Moorestown, NJ) and imaged with a Hitachi S-34000N VP-SEM (Hitachi, Placeton, CA).

Fluorescent Microscopy

Enucleated eyes were fixed in 10% formalin in phosphate buffer at pH 7.2 overnight, embedded in paraffin, and sectioned into 4 μm thick sections. Samples were stained with hematoxylin-eosin, and selected sections were analyzed with fluorescent microscopy with mounting media containing DAPI (4′,6 diamidino-2-phenylindole-2HCl) (Vector Laboratories, Burlingame, CA) following the manufacturer's instructions.

BrdU Labeling

To detect the potential proliferation in the RPE and inner retinal cells, we used 5-bromo-2′-dioxyuridine (BrdU) labeling, which integrates into the DNA of dividing cells.[31] Four eyes from four rabbits received line scanning laser using the same parameters as in the treatment protocol of this study at 4 days prior to enucleation. BrdU labeling reagent (10 mL; Invitrogen, Eugene, OR) was infused slowly into an ear vein 2 days and 1 day prior to animal sacrifice. Eyes and control samples from small intestines were fixed in formalin, embedded in paraffin, and sectioned into 4 to 5 μm thick sections. Sections were then incubated with anti-BrdU antibody and Texas Red secondary antibody (Santa Cruz Biotechnology, Santa Cruz, CA) following instructions of the manufacturer (Invitrogen). At least five sections of each sample were analyzed on fluorescent microscopy with mounting media containing DAPI.

Results

Following laser scanning, no ophthalmoscopically visible changes were detected except for the visible marker burns, as shown in Figure 1a. However, laser pattern was clearly visible in fluorescein angiography (FA) (Fig. 1b), which indicates damage to RPE. Acute histology (Fig. 1c) and TEM (Fig. 1d) revealed collapsed RPE cells and minor damage to outer segments of photoreceptors but no damage to choroid or

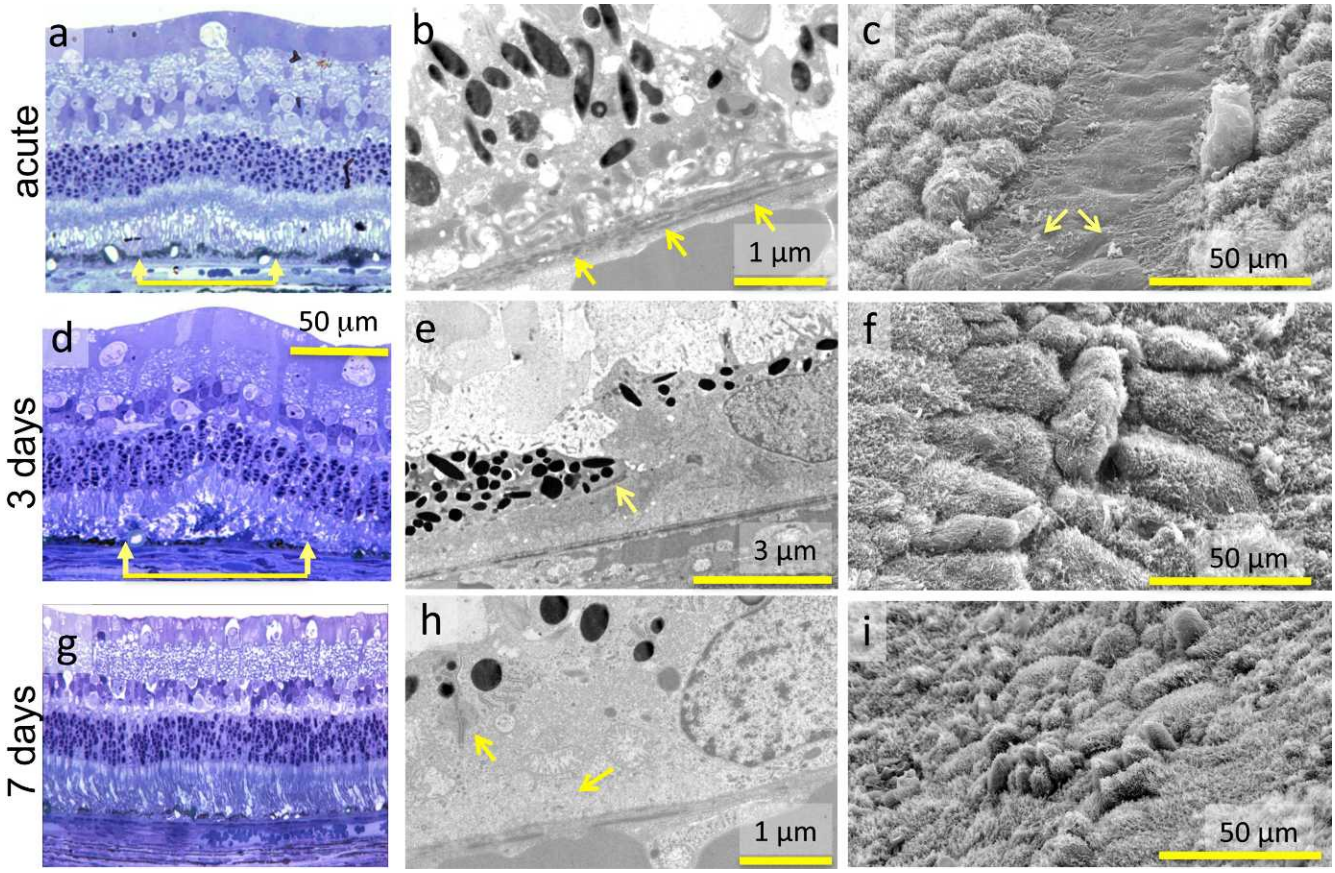

Figure 2. Healing of scanning laser lesions in the RPE and neurosensory retina. *Top row*: acute effects after laser. (**a**) Light microscopy (LM) 1 hour after laser shows collapse of RPE cells with limited damage (swelling) in the region of the photoreceptor outer segments. (**b**) TEM 1 hour after laser shows damaged RPE cells with disruption of cytoplasmic membranes, intracellular organelles, and basal infoldings. However, Bruch's membrane and choroid appear intact (*arrows*). (**c**) SEM 1 day after treatment shows an absence of RPE cells within the laser beam path. Surrounding RPE cells are sending foot processes into the damage zone (*arrows*). *Middle row*: 3 days after laser. (**d**) LM shows abnormal outer segments but no damage to the outer nuclear layer. (**e**) TEM shows the presence of tight junctions between two RPE cells (*arrow*), but a lack of basal infoldings above Bruch's membrane. (**f**) SEM demonstrates repopulation of the damaged area with large RPE cells. *Bottom row*: 7 days after laser. (**g**) LM shows normal retinal and RPE morphology, including the photoreceptor outer segments. (**h**) TEM demonstrates recovery of vertical tight junctions between RPE cells and normal basal infoldings and intracellular organelles (*arrows*). (**i**) SEM shows more complete restoration of the RPE monolayer with both large and small RPE cells, and with microvilli. *Arrows* in (**a**, **d**) show the length of the damage to the retinal pigment epithelium cells.

Bruch's membrane (Figs. 1c, 1d). SEM of RPE layer at 1 day after laser demonstrated lines empty of RPE cells (Fig. 1e).

Healing dynamics of the lesions is summarized in Figure 2. After 1 hour, RPE cells collapsed beneath the photoreceptors (Fig. 2a), with some overlying edema in the region of the photoreceptor outer segments. TEM (Fig. 2b) demonstrated RPE disruption with an intact Bruch's membrane underneath. After 1 day, SEM along the line of laser scanning showed an absence of the RPE cells on a smooth Bruch's membrane, and some initial cellular migration into the damage zone as indicated by RPE foot processes (Fig. 2c). Three days following laser application, the continuity of the RPE layer was reestablished (Fig. 2f); interestingly, cells appear stretched, suggesting migration rather than proliferation, at this stage. The photoreceptor outer segments remained disorganized and edematous, but the outer nuclear layer appeared intact (Fig. 2d). TEM showed partial resolution of the tight junctions between RPE cells, but did not show evidence of basal infoldings (Fig. 2d). After 7 days, the photoreceptor outer segments over the laser site appeared normal. Some of the RPE cells filling the defect were small with prominent apical processes, suggesting both cell division and proliferation mechanisms (Fig. 2i). Cell division was confirmed using a bromodeoxyuridine (BrdU) immunohistochemistry assay, which labels dividing cells and marked nearly half of the RPE cells in the treated areas (Fig. 3). At this time, TEM showed restoration of tight junctions and basal infoldings (Fig. 2h).

In order to evaluate downregulation of transgene expression, rAAV serotype 2 encoding GFP was administered to six pigmented rabbits. The vector was delivered via subretinal injection into two areas in each eye; balanced salt solution (BSS) vehicle was delivered to a third area as a control. Three weeks later, laser treatment was applied to one transfected bleb in each eye, with a line pattern density of 50% (i.e., laser lines were spaced one line width apart), as illustrated in Figure 1f. The same areas were then re-treated 4 weeks after the first laser treatment.

GFP expression was evaluated via fluorescence imaging. Whereas the BSS injection site showed only slightly elevated autofluorescence (Fig. 4a), transfected areas showed uniform fluorescence throughout the bleb (Figs. 4d, 4g). Areas treated with selective laser showed an overall decrease in fluorescence compared to nonlasered control areas, and gaps in fluorescence were visible marking the location of the laser scans (Fig. 4g). OCT showed normal photoreceptor morphology in all three areas, with outer segment markers such as the inner segment/outer segment junction line appearing intact (Figs. 4b, 4e, 4h). The laser-treated eye showed initial irregular

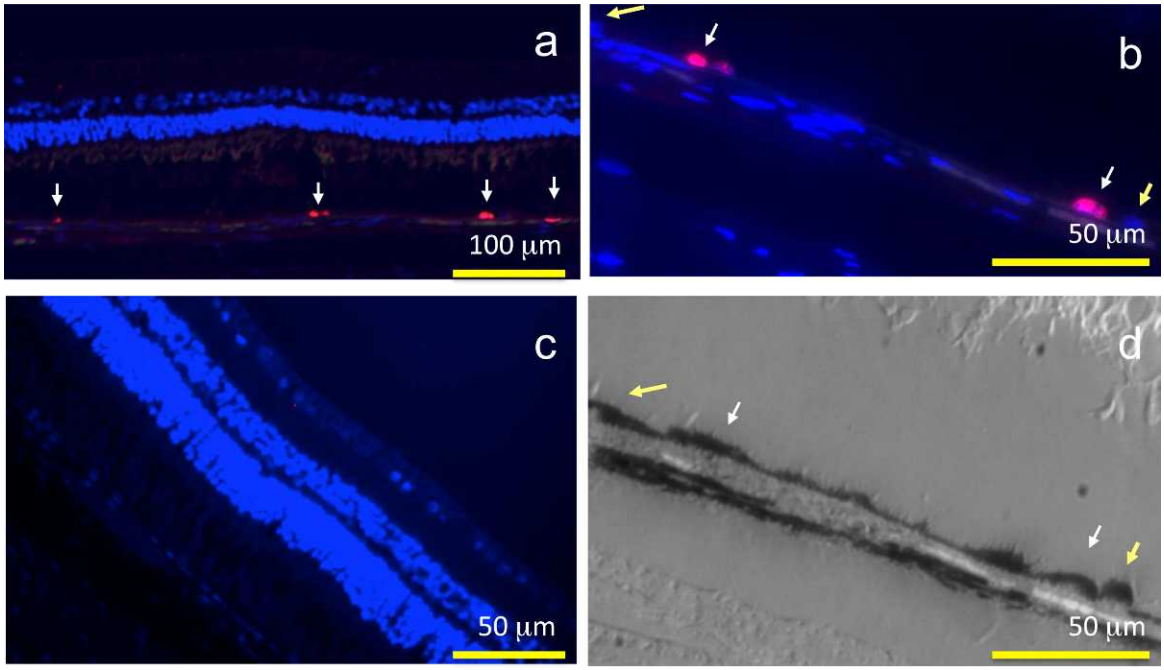

Figure 3. (**a**) Micrographs of BrdU (*red*) and DAPI (*blue*) immunostaining of the retina (×10 magnification) 4 days after laser treatment. BrdU-positive RPE cells are indicated by the *white arrows*. (**b**) BrdU (*red*) and DAPI (*blue*) immunostaining of the retina (×40 magnification) 4 days after laser treatment. BrdU-positive RPE cells are indicated by *white arrows*; BrdU-negative cells are indicated by *yellow arrows*. (**c**) BrdU immunostaining of nonlasered retina from the same animal does not show signs of BrdU uptake. (**d**) Hoffman contrast, white field image of the RPE layer in the same area as shown in (**b**).

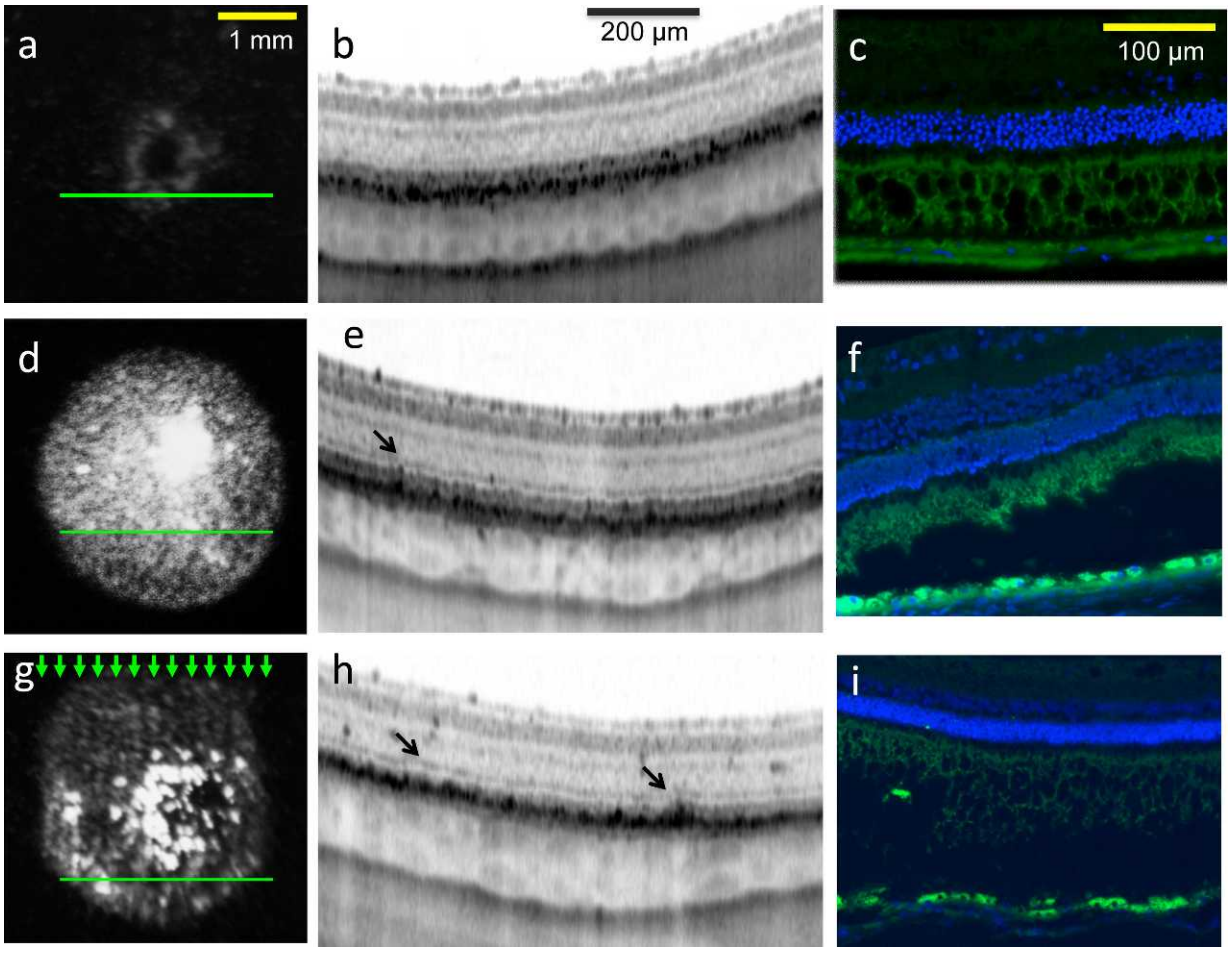

Figure 4. Relative findings in BSS, transfected control (nonlasered), and transfected treated (lasered) areas of retina. All images were obtained 1 month after the first laser treatment of the eye (7 weeks after retinal injections). BSS area (not transfected). (**a**) Fluorescence photography shows a

faint ring corresponding to mechanical RPE damage at the injection site. (**b**) OCT shows normal retina. (**c**) Fluorescent microscopy shows a modest (normal) background level of autofluorescence (*green*) in the RPE and outer segment region, and DAPI staining of the nuclei (*blue*). Control area (transfected, not lasered). (**d**) Fundus photography shows diffuse GFP fluorescence across the transfected area. (**e**) OCT shows normal morphology of the retina in the bleb area with an intact inner segment/outer segment junction line (*arrow*). (**f**) microscopy shows a uniform increase in RPE fluorescence, with no significant increase in the retinal fluorescence. Area transfected and treated with scanning laser. (**g**) The GFP-transfected bleb treated with laser shows vertical lines of decreased fluorescence as well as reduced total fluorescence, and *green arrows* illustrate a pattern of the line scanning laser applied. (**h**) OCT in the laser-treated area shows some focal sites with increased reflectivity in the RPE, but no damage to the outer retina or inner segment/outer segment junction (*arrows*). (**i**) Microscopy of the lasered RPE shows interposed areas of enhanced and decreased RPE fluorescence (with no increased fluorescence in the neurosensory retina). *Green lines* (**a**, **d**, **g**) represent where the laser was applied.

thickening of RPE cells (Fig. 4h). Histologic sections of the BSS area 1 month after laser (Fig. 4c) showed mild background autofluorescence of the RPE and photoreceptors. In contrast, the transfected control area (Fig. 4f) had continuous GFP expression throughout the RPE layer. In the laser-treated area (Fig. 4i), the RPE showed irregular loss of fluorescence with some cells bright and others dark, presumably from the expected pattern of selective laser treatment, corresponding to the pattern in Figure 4g.

The time course of GFP expression and the effect of selective laser treatment on transgene expression are plotted in Figure 5. The transfected areas reached maximum fluorescence level at 3 to 4 weeks and remained stable throughout the follow-up period in the control (nonlasered) eyes. To allow comparison of the total fluorescent signal from transfected areas of various sizes, the signals from each area were normalized to their expression at 21 days (the time of laser treatment). Figure 5B depicts the ratio of the average fluorescent signal (excluding background autofluorescence) from the laser-treated areas versus the control (nontreated) areas. In the areas treated with line pattern of 50% density, the signal decreased by 54% within 1 week and remained stable for 4 weeks. At that time, the same area was re-treated, again using 50% pattern density. This resulted in an additional 48% reduction, bringing the total signal to 26% of its original level, which remained stable for the last 3 weeks of the follow-up. In vivo imaging and ultrastructural analysis with TEM and SEM after the second treatment confirmed a lack of damage to the

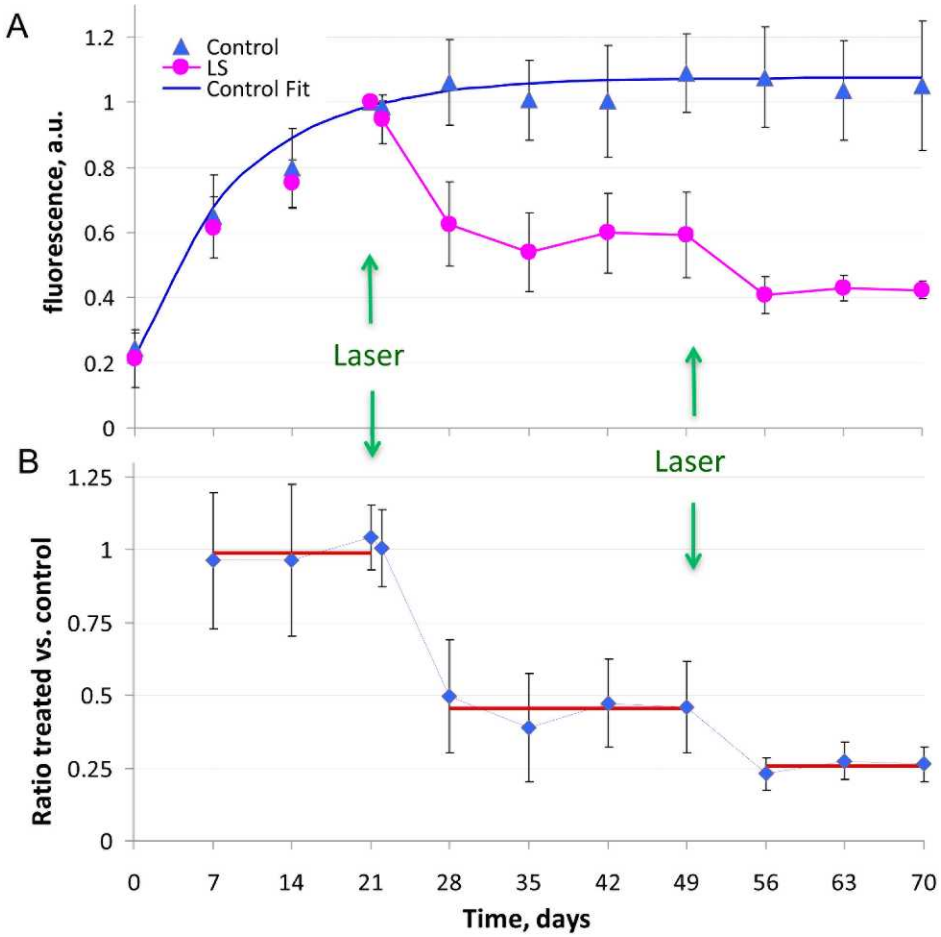

Figure 5. Fluorescence measurements from transfected areas, treated and not treated (control) with line-scanning laser (LS). (**A**) Average fluorescence of the transfected areas over time, normalized to its maximum at 3 weeks. The *solid blue line* (control fit) is an exponential curve fit to the transfected (untreated areas) data. Retinal areas treated at 3 and 7 weeks demonstrated step reductions in fluorescence signal. (**B**) Ratio of the fluorescent signals (excluding background fluorescence) from the LS versus control blebs. *Solid lines* show average brightness ratio over the period before the laser and after each laser treatment.

neurosensory retina or Bruch's membrane, as well as a pattern of RPE repair similar to that after the first treatment.

Discussion

Despite great efforts in the creation of inducible gene expression systems, the developed approaches have been cumbersome and provide an incomplete solution to most clinical settings. The most widely used systems, such as Tet-On, Tet-Off, rapamycin-induced dimerization, and steroid-hormone regulation, require that a drug be taken on a constant basis to maintain expression in the "on" or "off" state.[11,12] The small-molecule agent used for induction may itself have undesirable effects, such as off-target biological effects of rapamycin, like immunosuppression, and off-target effects of steroid hormones, which would be similar to hormone-replacement therapy effects at the levels proposed for the RU-486 system.[15] Systems that seem to avoid this problem, such as the Tet-On system, suffer from other shortcomings that prevent widespread clinical use, such as documented immune response to the gene product in large animals.[17] Another shortcoming is that these systems are often "leaky," leading to a low level of background expression persisting in the "off" state. Finally, for such a system to reach widespread clinical use, substantial barriers would need to be overcome in the clinical trial design phase of drug development; such an approach would necessitate independent arms to demonstrate safety of the gene therapy agent alone, the inducible agent alone, and the combination, and in the later phases would need to employ a randomization scheme to switch off the therapy. The latter poses an ethical challenge, and using the switch only "when needed" is problematic analytically. These challenges perhaps summarize why no regulatable system has been employed in a human clinical trial to date,[12] and suggest that new technology is needed in this field.

Clinical acceptance of retinal gene therapy would be enhanced by availability of techniques to regulate transgene expression in the RPE without damage to the neural retina. The ideal system would not require an inducer agent, would act only locally at the site of transduction, and would allow gradual reduction of transgene expression to a desired amount. In the present study, we have demonstrated that rapid laser scanning can achieve these criteria, and the same area can be scanned repeatedly without any measurable adverse effect.

Following AAV-mediated gene delivery, the transgene is not replicated during cell division and the vector is lost in dividing cells; thus, when stimulated to proliferate, RPE cells do not duplicate the transgene-bearing vector cassette. Therefore, selective destruction of RPE cells reduces the total amount of secreted protein even when the remaining RPE cells migrate or proliferate to restore functional continuity of the RPE layer. Selectively damaging a designated fraction of transfected RPE cells reduces the amount of expressed transgene proportionally, so that the density of the scanning laser pattern controls dosimetry of downregulation.

It has been shown that microsecond pulses can produce intracellular microbubbles around light-absorbing melanosomes, leading to selective death of RPE cells while the surrounding retinal temperature remains sublethal.[18] Selective RPE destruction without photoreceptor damage was initially achieved with an Nd:YLF laser using 1.7 μs pulse durations.[36,37] OCT imaging in human patients has demonstrated unaffected neural retina and RPE thinning at 1 hour and normal neural retina and RPE at 1 year. SRT (selective therapy of the RPE) with microsecond pulses has been tested clinically for diabetic macular edema and central serous chorioretinopathy and was shown to be safe and effective.[37–40] At energies corresponding to selective damage of the RPE, no immediate ophthalmoscopically visible retinal lesions are produced. Instead of use of a dedicated microsecond laser, sufficiently short exposures can also be produced by rapid scanning of a continuous laser,[20,21,41] the method used in our study. Many retinal scanning lasers currently on the market could be adapted to perform such treatment, which will enable immediate access to this technology worldwide.

It has been demonstrated that even if the photoreceptors have been locally damaged by photocoagulation in narrow lesions, the normal anatomy of the photoreceptor layer is restored over time due to migration of the photoreceptors into the lesion.[20,42,43] Experiments with multielectrode arrays in vitro[44] and microperimetry tests in vivo[45] have shown that in these cases, retinal sensitivity is restored as well. In our case the photoreceptors are not destroyed; just their outer segments detach above the damaged RPE, and as soon as RPE cells are back, the outer segments become normal. Therefore, we do not anticipate any loss of retinal functionality.

If this approach is proven clinically successful, it could be directly applied to programs that utilize rAAV vectors to transfect RPE cells, including those using anti-VEGF agents for treatment of neovascular AMD, diabetic retinopathy, and macular edema. The use of a chronic "biofactory" approach could alleviate the financial and organizational burden of monthly injections. The possibility of decreasing the transgene expression, if necessary, by laser therapy could reduce potential concerns associated with irreversibility of the gene therapy and thereby would enhance its clinical adoption.

The selectivity of this method with respect to RPE cells, however, also points to a limitation, since it would not be expected to alter transgene expression in other cell types. Nevertheless, this technology may provide a useful adjunct to clinical approaches that target RPE cells, which have shown promise in previous and ongoing gene therapy clinical studies.

References

1. Sheridan C. Gene therapy finds its niche. *Nat Biotechnol*. 2011;29:121–128.
2. Maguire AM, Simonelli F, Pierce EA, et al. Safety and efficacy of gene transfer for Leber's congenital amaurosis. *N Engl J Med*. 2008;358:2240–2248.
3. Hauswirth WW, Aleman TS, Kaushal S, et al. Treatment of leber congenital amaurosis due to RPE65 mutations by ocular subretinal injection of adeno-associated virus gene vector: short-term results of a phase I trial. *Hum Gene Ther*. 2008;19:979–990.
4. Bainbridge JWB, Smith AJ, Barker SS, et al. Effect of gene therapy on visual function in Leber's congenital amaurosis. *N Engl J Med*. 2008;358:2231–2239.
5. Lai CM, Estcourt MJ, Himbeck RP, et al. Preclinical safety evaluation of subretinal AAV2.sFlt-1 in non-human primates. *Gene Ther*. 2012;19:999–1009.
6. Lukason M, DuFresne E, Rubin H, et al. Inhibition of choroidal neovascularization in a nonhuman primate model by intravitreal administration of an AAV2 vector expressing a novel anti-VEGF molecule. *Mol Ther*. 2011;19:260–265.
7. Liu MM, Tuo J, Chan CC. Gene therapy for ocular diseases. *Br J Ophthalmol*. 2011;95:604–612.
8. Friedman DS, O'Colmain BJ, Muñoz B, et al. Prevalence of age-related macular degeneration in the United States. *Arch Ophthalmol*. 2004;122:564–572.
9. Bressler NM. Antiangiogenic approaches to age-related macular degeneration today. *Ophthalmology*. 2009;116:S15–S23.

10. Klein RJ, Zeiss C, Chew EY, et al. Complement factor H polymorphism in age-related macular degeneration. *Science*. 2005;308:385–389.
11. Stieger K, Belbellaa B, Le Guiner C, et al. In vivo gene regulation using tetracycline-regulatable systems. *Adv Drug Deliv Rev*. 2009;61:527–541.
12. Goverdhana S, Puntel M, Xiong W, et al. Regulatable gene expression systems for gene therapy applications: progress and future challenges. *Mol Ther*. 2005;12:189–211.
13. Guo ZS, Li Q, Bartlett DL, et al. Gene transfer: the challenge of regulated gene expression. *Trends Mol Med*. 2008;14:410–418.
14. Pollock R, Issner R, Zoller K, et al. Delivery of a stringent dimerizer-regulated gene expression system in a single retroviral vector. *Proc Natl Acad Sci U S A*. 2000;97:13221–13226.
15. Wang Y, OMalley BW, Tsai SY, O'Malley BW. A regulatory system for use in gene transfer. *Proc Natl Acad Sci U S A*. 1994;91:8180–8184.
16. No D, Yao TP, Evans RM. Ecdysone-inducible gene expression in mammalian cells and transgenic mice. *Proc Natl Acad Sci U S A*. 1996;93:3346–3351.
17. Le Guiner C, Stieger K, Snyder RO, et al. Immune responses to gene product of inducible promoters. *Curr Gene Ther*. 2007;7:334–346.
18. Schuele G, Rumohr M, Huettmann G, Brinkmann R. RPE damage thresholds and mechanisms for laser exposure in the microsecond-to-millisecond time regimen. *Invest Ophthalmol Vis Sci*. 2005;46:714–719.
19. Blumenkranz MS, Yellachich D, Andersen DE, et al. Semi-automated patterned scanning laser for retinal photocoagulation. *Retina*. 2006;26:370–376.
20. Paulus YM, Jain A, Nomoto H, et al. Selective retinal therapy with microsecond exposures using a continuous line scanning laser. *Retina*. 2011;31:380–388.
21. Framme C, Alt C, Schnell S, et al. Selective targeting of the retinal pigment epithelium in rabbit eyes with a scanning laser beam. *Invest Ophthalmol Vis Sci*. 2007;48:1782–1792.
22. Lai CM, Yu MJ, Brankov M, et al. Recombinant adeno-associated virus type 2-mediated gene delivery into the Rpe65-/- knockout mouse eye results in limited rescue. *Genet Vaccines Ther*. 2004;2:3.
23. Lai C, Shen W, Brankov M, et al. Long-term evaluation of AAV-mediated sFlt-1 gene therapy for ocular neovascularization in mice and monkeys. *Mol Ther*. 2005;12:659–668.
24. Lebherz C, Maguire A, Tang W, et al. Novel AAV serotypes for improved ocular gene transfer. *J Gene Med*. 2008;10:375–382.
25. Lai YK, Shen WY, Brankov M, et al. Potential long-term inhibition of ocular neovascularisation by recombinant adeno-associated virus-mediated secretion gene therapy. *Gene Ther*. 2002;9:804–813.
26. Paskowitz DM, Greenberg KP, Yasumura D, et al. Rapid and stable knockdown of an endogenous gene in retinal pigment epithelium. *Hum Gene Ther*. 2007;18:871–880.
27. Acland GM, Aguirre GD, Ray J, et al. Gene therapy restores vision in a canine model of childhood blindness. *Nat Genet*. 2001;28:92–95.
28. Amado D, Mingozzi F, Hui D, et al. Safety and efficacy of subretinal readministration of a viral vector in large animals to treat congenital blindness. *Sci Transl Med*. 2010;2:21ra16.
29. Bennicelli J, Wright JF, Komaromy A, et al. Reversal of blindness in animal models of leber congenital amaurosis using optimized AAV2-mediated gene transfer. *Mol Ther*. 2008;16:458–465.
30. Provost N, Le Meur G, Weber M, et al. Biodistribution of rAAV vectors following intraocular administration: evidence for the presence and persistence of vector DNA in the optic nerve and in the brain. *Mol Ther*. 2005;11:275–283.
31. Bennett J, Ashtari M, Wellman J, et al. AAV2 gene therapy readministration in three adults with congenital blindness. *Sci Transl Med*. 2012;4:120.
32. Maguire A, Simonelli F, Pierce E, et al. Safety and efficacy of gene transfer for Leber's congenital amaurosis. *N Engl J Med*. 2008;358:2240–2248.
33. Hauswirth W, Aleman T, Kaushal S, et al. Treatment of leber congenital amaurosis due to RPE65 mutations by ocular subretinal injection of adeno-associated virus gene vector: short-term results of a phase I trial. *Hum Gene Ther*. 2008;19:979–990.
34. Bainbridge J, Smith A, Barker S, et al. Effect of gene therapy on visual function in Leber's congenital amaurosis. *N Engl J Med*. 2008;358:2231–2239.
35. Peden MC, Min J, Meyers C, et al. Ab-externo AAV-mediated gene delivery to the suprachoroidal space using a 250 micron flexible microcatheter. *PloS One*. 2011;6:e17140.
36. Brinkmann R, Huttmann G, Rogener J, et al. Origin of retinal pigment epithelium cell damage by pulsed laser irradiance in the nanosecond to microsecond time regimen. *Lasers Surg Med*. 2000;27:451–464.
37. Brinkmann R, Roider J, Birngruber R. Selective retina therapy (SRT): a review on methods, techniques, preclinical and first clinical results. *Bull Soc Belge Ophtalmol*. 2006;302:51–69.
38. Elsner H, Porksen E, Klatt C, et al. Selective retina therapy in patients with central serous chorioretinopathy. *Graefes Arch Clin Exp Ophthalmol*. 2006;244:1638–1645.
39. Elsner H, Klatt C, Liew SH, et al. Selective retina therapy in patients with diabetic maculopathy. *Ophthalmologe*. 2006;103:856–860.
40. Roider J, Brinkmann R, Wirbelauer C, et al. Subthreshold (retinal pigment epithelium) photocoagulation in macular diseases: a pilot study. *Br J Ophthalmol*. 2000;84:40–47.
41. Brinkmann R, Koop N, Ozdemir M, et al. Targeting of the retinal pigment epithelium (RPE) by means of a rapidly scanned continuous wave (CW) laser beam. *Lasers Surg Med*. 2003;32:252–264.
42. Paulus YM, Jain A, Gariano RF, et al. Healing of retinal photocoagulation lesions. *Invest Ophthalmol Vis Sci*. 2008;49:5540–5545.
43. Belokopytov M, Belkin M, Dubinsky G, et al. Development and recovery of laser-induced retinal lesion in rats. *Retina*. 2010;30:662–670.
44. Sher A, Leung L-S, Leng T, et al. Retinal plasticity and restoration of function after photocoagulation. *Invest Ophthalmol Vis Sci*. 2010;51:2482.
45. Merigan WH, Strazzeri J, DiLoreto DA Jr, et al. Visual recovery after outer retinal damage in the macaque. *Invest Ophthalmol Vis Sci*. 2011;52:3202.